fortune Journals

Research Article

JOURNAL OF ORTHOPAEDICS AND SPORTS MEDICINE

ISSN: 2688-5115

Inflammation and Fatty Infiltration Correlates with Rotator Cuff Muscle Atrophy in Hypercholesterolemic Yucatan Microswine

Hoangvi Le, Vikrant Rai, Devendra K. Agrawal*

Abstract

Rotator cuff injuries are the most common injuries among active and training astronauts. According to the CDC, 1 in 4 adults in the U.S. experience rotator cuff injuries, particularly affecting the supraspinatus muscle. Hypercholesterolemia, a condition characterized by high levels of LDL cholesterol, is prevalent in approximately 2 in 5 adults in the US and is a risk factor for worsened outcomes in shoulder inflammation and rotator cuff injury repairs. Chronic inflammation, a prolonged low-grade inflammatory state, can arise from conditions like hypercholesterolemia and contribute to muscle atrophy. Skeletal muscle atrophy can be caused by factors such as disuse, aging, malnutrition, and microgravity, and currently lacks approved drug therapies. Thus, gaining a comprehensive understanding of the associations between hypercholesterolemia, chronic inflammation, and skeletal muscle atrophy is imperative for developing effective strategies to manage this condition. We conducted an animal study in Yucatan miniswine to investigate the impact of a high-cholesterol diet on rotator cuff muscle. The results suggested the presence of chronic inflammation in rotator cuff muscle hypercholesterolemic swine, associated with elevated pro-inflammatory cytokines and intramuscular adipocytes, and skeletal muscle atrophy. The results also revealed upregulation of the FOXO3/TRIM63/Titin axis in a hyperlipidemic state. These findings open new perspectives for developing better treatment strategies by targeting the FOXO3/TRIM63/Titin axis to manage rotator cuff muscle atrophy in the context of hypercholesterolemia.

Keywords: Hypercholesterolemia; Muscle atrophy; Rotator cuff muscles; Chronic inflammation; Titin degradation

Introduction

Compared to activities done safely inside the International Space Station (ISS), spacewalks are considered one of the most dangerous jobs in mankind and can certainly contribute to the physical and psychological stress of astronauts. In August 2021, the NASA Office of Inspector General performed an audit to examine the current progress of the next-generation spacesuits for the ISS and Artemis missions [1]. This audit also revealed the health-related risks associated with the current spacesuit and examples of negative health outcomes from specific missions. Spacesuit-related risks include decompression sickness, thermal regulation, shoulder injuries, hand injuries, malnutrition, and dehydration. Extravehicular activity (EVA) injuries of hands and shoulders are usually sustained with the EMU spacesuit during spacewalks and EVA training. However, rotator cuff injuries are the most common among active and training astronauts [2,3]. In zero gravity,

Affiliation:

[1]Department of Translational Research, College of Osteopathic Medicine of the Pacific, Western University of Health Sciences, Pomona, California USA

***Corresponding Author:**

Devendra K Agrawal, Department of Translational Research, College of Osteopathic Medicine of the Pacific, Western University of Health Sciences, Pomona, California USA.

Citation: Hoangvi Le, Vikrant Rai, Devendra K Agrawal. Inflammation and Fatty Infiltration Correlates with Rotator Cuff Muscle Atrophy in Hypercholesterolemic Yucatan Microswine. Journal of Orthopedics and Sports Medicine. 6 (2024): 198-214.

Received: August 11, 2024
Accepted: September 06, 2024
Published: September 16, 2024

Hoangvi Le, et al., J Ortho Sports Med 2024
DOI:10.26502/josm.511500161

astronauts tend to use their upper extremities for movement and physical tasks, versus their lower extremities, resulting in the overuse of shoulders and hands. The spacesuit hardware of the upper torso was the main cause of injury during active duty [2]. However, rotator cuff injuries have only increased recently in the National Aeronautics and Space Administration (NASA), perhaps due to the changes in space suit design or changes in the spaceflight requirements (i.e. all astronauts must be EVA certified starting in 2000) [4]. Astronauts selected in the 1990's have higher incidences of shoulder surgery. Astronauts who have performed more than five spacewalks were twice as likely to sustain shoulder injuries than astronauts who performed one spacewalk [5].

Shoulder injury is a broad term that encompasses many different types of myopathies or tendinopathies relating to the shoulder rotator cuff. Rotator cuff injury could manifest from hypercholesterolemia due to higher levels of total cholesterol, triglycerides, and LDL cholesterol [6-9]. Dyslipidemia and muscle atrophy are associated with the failure of rotator cuff repairs and increased risk of retear [8-12]. However, the underlying molecular pathways involved in muscle and tendon injuries contributing to RCI are yet to be fully understood. It should also be noted that astronauts also develop hypercholesterolemia contributing to cardiovascular diseases [13]. However, the current collection of space-related biomedical research on hypercholesterolemia is insufficient and does not reveal much about the effect of microgravity on astronauts' cholesterol [14]. Cholesterol is not a routine measurement for astronauts when landing [14] and measuring HDL, LDL, triglycerides, and lipoprotein levels is important because levels change during space mission and after spaceflight [15]. If the pursuit of space travel is continued, additional research is necessary to develop enhanced treatments for EVA-associated rotator cuff injuries in addition to addressing microgravity-induced change in cholesterol levels and its effects on muscle atrophy.

Skeletal muscles are highly adaptable and can undergo hypertrophy (increase in muscle mass) or atrophy (decrease in muscle mass) in response to changes in physical activity levels or other factors such as aging or disease [16,17]. The ability of skeletal muscles to generate significant force and power is crucial for human athletic performance and essential for activities of daily living. Overall, skeletal muscle contributes significantly to metabolic homeostasis, and alterations in its metabolism have been correlated with various metabolic disorders, including insulin resistance, type 2 diabetes, and obesity [18,19]. Sustaining healthy skeletal muscle function through exercise and other lifestyle modifications is vital for overall metabolic health. Skeletal muscle atrophy is a condition characterized by muscle wasting or when protein degradation exceeds protein synthesis [20]. The plasticity of skeletal muscle is widely studied by experts and weight trainers alike in the scope of muscle hypertrophy by exploiting mechanisms to increase myofiber regeneration [21-23]. However, muscle atrophy remains incompletely elucidated due to its common acknowledgment as a condition to be proactively avoided because diminished muscle mass and strength are risk factors associated with disability and mortality [24].

Metabolic studies have shown a growing interest in how excess or deficiencies in cholesterol could impact the homeostasis of skeletal muscle [25-27]. Excess serum cholesterol, or hypercholesterolemia, is prevalent in metabolic disorders (i.e. obesity, diabetes, malnutrition), peripheral atherosclerosis, cancer, and aging [28,29]. Cholesterol depletion induced by statin drugs may exacerbate muscle atrophy [30]. Altered lipid metabolism plays a role in skeletal muscle weakness, as shown in obesity-like disease models. In rats, a short-term high fat diet impaired function in oxidative-type skeletal muscles [31]. For patients with spinal muscular atrophy (SMA), malnutrition is a major concern because of defects in fatty acid transport and mitochondrial β-oxidation [32,33]. In addition to altered lipid metabolism, glucose metabolism alteration may cause skeletal muscle atrophy, as observed in diabetes [34]. Too much cholesterol can cause negative effects on important skeletal muscle membrane-protein species, such as those found in the transverse tubule, or t-tubule. The t-tubule is considerably more cholesterol-rich than the sarcolemma and increasing this level further impedes the trafficking of intracellular glucose transporter, GLUT4, to the t-tubule and other surface membranes [35,36]. Cholesterol and hydration play a critical role in cell membrane fluidity and are directly correlated with each other [37]. This is demonstrated by increased serum cholesterol concentration in blood tests in dehydrated patients [38]. Dehydration can lead to hypertension, muscle fatigue, and dizziness [39-41]. This suggests that hypercholesterolemia, through inflammation and fatty infiltration, can promote skeletal muscle atrophy. A study has demonstrated that intramuscular adipose tissue directly obstructs skeletal muscle contractions [42]. Although obesity is often associated with hypercholesterolemia, patients with anorexia nervosa can also develop hypercholesterolemia and experience muscle atrophy due to malnutrition [43].

Rotator cuff muscle atrophy is also a common condition that can result in significant shoulder pain and disability. It is characterized by a loss of muscle mass and muscle weakness in the rotator cuff muscles including subscapularis, teres minor, supraspinatus, and infraspinatus. Recent research has shown that hypercholesterolemia may play a role in the development of rotator cuff muscle atrophy [44]. High levels of cholesterol have been associated with changes in muscle composition and function, including reduced muscle fiber size and impaired muscle regeneration [45]. Furthermore, high cholesterol levels have been linked to insulin resistance,

Hoangvi Le, et al., J Ortho Sports Med 2024
DOI:10.26502/josm.511500161

inflammation, and oxidative stress, all of which can contribute to muscle atrophy. Insulin resistance can impair muscle protein synthesis and promote muscle breakdown, while chronic inflammation and oxidative stress can lead to muscle damage and impair muscle regeneration [18]. This study aims to investigate the effect of hypercholesterolemia on muscle atrophy involving muscle protein degradation. We hypothesize that hypercholesterolemia-induced chronic inflammation and oxidative stress will increase titin protein degradation and result in muscle atrophy.

Materials and Methods

The rotator cuff muscle tissues (supraspinatus) were collected from hypercholesterolemic Yucatan microswine and control tissue samples were collected from Yucatan miniswine fed with normal diet being used in other studies. For the hypercholesterolemic group, female microswine aged 4-5 months (25–30 kg) kept at the animal facility of Western University of Health Sciences, Pomona, California, with a 12 h light and dark cycle at 72–74 °F and cared for per National Institute of Health standards were used (R19IACUC026). The swine were fed for 1 year with a hypercholesterolemic atherogenic diet purchased from Research Diets Inc (RDI) (NJ, USA) at Sinclair Bio-resources before transferring to our animal facility. RDI's high-cholesterol diet (#D17012601) contains 51% carbohydrates, 20% protein, 10% fat, and 4% cholesterol. For the control group, female Yucatan miniswine aged 4-5 months (20–30 kg) fed with the Mini-Pig Grower Diet (Test Diet # 5801) and allowed to drink water ad libitum were used (R20IACUC038). After 1 year, tissues from a total of 14 Yucatan swine, n=7 microswine (high cholesterol diet) and n=7 miniswine (normal diet), were collected for rotator cuff tissue histology and primary skeletal muscle cell isolation. Blood was collected for biochemical analysis and the total cholesterol levels in Yucatan microswine were in the range of 450-700 mg/dl while in Yucatan miniswine, the levels were in the range of 80-120 mg/dl.

Tissue Harvesting and Processing

The supraspinatus muscle of the rotator cuff was harvested after euthanasia and divided into three parts for histological studies (stored in 10% formalin at room temperature), RNA isolation (stored in RNA*later*™, -80°C), and protein isolation (stored at -80°C). Formalin-fixed supraspinatus muscle samples were prepared in standard cassettes and processed with the Sakura Tissue Tek VIP E300 Programmable Infiltration Tissue Processor. Processed tissue cassettes were transferred to the TN1700 Embedding Center to be embedded onto metal-based molds and cooled on a 5°C cooling plate. Formalin-fixed, paraffin-embedded (FFPE) tissue blocks were sectioned at 5µm using a tungsten carbide knife in a Leica RM2265 rotary microtome (LeicaTM, Germany). Sectioned tissue pieces were attached to positively charged glass slides and baked at 60°C for 60 minutes and later used for histology and immunostaining.

Hematoxylin and Eosin and Masson's Trichrome staining

Tissue sections were deparaffinized, rehydrated, stained, washed with deionized (DI) water, dehydrated, and finally dried for coverslip mounting. For Hematoxylin and eosin, tissues were stained in hematoxylin for 1 minute, washed for 3 minutes, dipped in Bluing reagent 10 times, then stained in Eosin for 3 minutes. For Masson's Trichrome, tissues were stained in Bouin's solution for 1 hour at 56°C, washed in running water until the yellow color dispersed, stained in Wiegert iron hematoxylin for 10 minutes, rinsed with warm running water for 5 minutes, washed in DI water for 2 minutes, then stained in Biebrich scarlet-acid fuchsin for 6 minutes, washed in DI water for 3 minutes, then stained in phosphomolybdic-phosphotungstic acid for 10 minutes, and immediately transferred into aniline blue for 6 minutes, then washed in 1% acetic acid twice for 2 minutes. All stained tissues were scanned with a Leica DM6 B Upright Microscope at a scale of 100µm. Three to four random images were captured from each section and three sections from each swine were scanned for each protein of interest.

Immunohistochemistry

For immunohistochemistry (IHC), sections were deparaffinized and rehydrated similarly as described before. Antigen retrieval was done in 1% citrate buffer at 95°C for 30 minutes and cooled before washing. Tissues were circled with a pap pen and incubated in 3% hydrogen peroxide for 15 minutes. Tissue sections were incubated with blocking serum (from Vectastain) for 1 hour at room temperature. After tipping off the blocking solution, tissue sections were incubated with primary antibodies (Table 1) overnight at 4°C and washed three times with 1X PBS following incubation. Then, the tissue sections were incubated with secondary antibodies for 1 hour at room temperature, and tissue sections were washed three times with 1X PBS. ABC solution from VECTASTAIN Elite ABC Kit, Peroxidase for either Rabbit IgG (PK-6101), Mouse IgG (PK-6102), or Goat IgG (PK-6105) was used to incubate tissue sections for 30 minutes. After washing, chromogen detection used was DAB (Thermo Scientific 34002) or AEC (Vector Laboratories SK-4200). Negative staining controls were stained with non-immune IgG antibody, Donkey anti-Rabbit IgG (H+L), HRP, with only primary antibody, and with only secondary antibody. Triplicates for each antibody and tissue combination were imaged at 100µm for ImageJ analysis. Average stained intensity (average intensity of the color) was measured using the Color Deconvolution 2, an ImageJ plug-in [46]. Three to five images from each stained tissue section were scanned for analysis.

Hoangvi Le, et al., J Ortho Sports Med 2024
DOI:10.26502/josm.511500161

Table 1: Primary Antibodies with their respective dilution factors used for immunostaining.

Antibody	Dilution	Catalog#	Antibody	Dilution	Catalog#
Adiponectin	1:400	ab126611	IL-1Ra	1:50	sc8481
CD163	1:100	ab87099	IL-6	1:50	ab6672
CD206	1:200	ab64693	LDLR	1:100	ab52818
CD68	1:100	ab125212	LEP	1:100	ab16227
CD86	1:100	ab269587	MCP-1	1:100	ab9669
COL-1	1:200	ab6308	MuRF1	1:200	PA5-76695
COL-3	1:200	ab7778	Myogenin	1:200	NB100-5651
FOXO3	1:200	NB100-614	TNF-α	1:200	ab6671
IL-10	1:200	ab9969	TTN	1:100	NB600-1206
IL-1β	1:200	ab156791			

Real-Time qPCR

Total RNA was isolated from rotator cuff tissues and isolated primary cells using Trizol. The total RNA was diluted with 10µL of RNA/DNAase-free water and stored at -80°C until measured with NanoDrop for the yield of RNA. 1µl of diluted RNA concentration was measured using 260/280 and values between 1.8–2.0 were acceptable. To make cDNA, Bio-Rad iScript cDNA Synthesis Kit (#1708891) was used to make a 20µL cocktail and amplified with the Bio-Rad T100 Thermal Cycler (Volume: 20µL, 25°C for 5 minutes, 46°C for 20 minutes, 95°C for 1 minute, and stored at 4°C indefinitely). The cDNA concentration was measured with NanoDrop again and diluted as needed. For each sample, 3 µL (15ng) of cDNA was mixed with 7 µL of master mix cocktail for each gene of interest (1 µL forward primer, 1 µL reverse primer, and 5 µL of SYBR green) for a total of 10µL and was triplicated in a 96 well PCR plate. Forward and reverse primer nucleotide sequences are listed in Table 2. PCR was conducted using BioRad CF96 Thermal Cycler with 39 cycles. The cycling conditions were 3 min at 95°C for initial denaturation, 39 cycles of 15s at 95°C, and 15s at 55–60°C (according to the primer annealing temperatures) followed by melting curve analysis. Cq values were compiled to calculate delta-delta-CT ($2^{-\Delta\Delta CT}$) to compare fold change and statistical significance was calculated using a two-sided t-test. The primers for different genes in swine (Table 1) were obtained from Integrated DNA Technologies (Coralville, IA, USA). Normalization for relative mRNA expression was evaluated with housekeeping gene, 18S.

Table 2: Forward and reverse nucleotide sequences for genes of interest used in this study for RT-qPCR.

Gene Name	Forward	Reverse
CD68	5'-TCCCAGTGACCAAACCATCC-3'	5'-TTGGAACAGATGCTCACGGA-3'
CD86	5'-GTTGTGTGTGGGATGGTGTC-3'	5'-GTTTGTTCACTCGCCTTCCTG-3'
CD206	5'-TAGGGGTGCCCTCAAAAACC-3'	5'-GCGTGTCATTTCTGCACTCC-3'
CD163	5′-CTGTGATGATGGCTGGGATAG-3'	5′-AATGTGTCCAGTTCCCTCAC-3'
IL-6	5'-TGCAGTCACAGAACGAGTGG-3'	5'-CAGGTGCCCCAGCTACATTAT-3'
TNF-α	5'-CATCTACCTGGGAGGGGTCT-3'	5'-CCAGATAGTCGGGCAGGTTG-3'
IL-1β	5′-ATGGACAAGCTGAGGAAGATG-3′	5′-CCCATGTGTCGAAGAAGATAGG-3′
MCP-1	5′-AAACGGAGACTTGGGCACAT-3′	5′-CTTGCAAGGACCCTTCCGTC-3′
ADIPOQ	5′-TTGAAGGTCCCCGAGGTTTC-3′	5′-GAACGGTAGACATAGGCGCT-3′
LEP	5′-CTTCATCCCTGGGCTCCATC-3′	5′-GGCAGACTGGTGAGGATCTG-3′
MYOD1	5′-GCTCCGCGACGTAGATTTGA-3′	5′-GGAGTCGAAACACGGGTCAT-3′
FOXO3	5′- ACAAACGGCTCACTCTGTCC-3′	5′-GTTGCTGTCGCCCTTATCCT-3′
TRIM63	5′-TCTTCCAGGCTGCAAATCCC-3′	5′-GTGACGGTCCATGATCACCT-3′
TTN	5′-AAGCGACTGATTGGGGAGTTG-3′	5′-GGCTTGGTTCGCTAAGTCCA -3′
18s	5'-CCCACGGAATCGAGAAAGAG-3'	5'-TTGACGGAAGGGCACCA-3'

Citation: Hoangvi Le, Vikrant Rai, Devendra K Agrawal. Inflammation and Fatty Infiltration Correlates with Rotator Cuff Muscle Atrophy in Hypercholesterolemic Yucatan Microswine. Journal of Orthopedics and Sports Medicine. 6 (2024): 198-214.

Table 3: List of primary and secondary antibodies with dilutions used for Western blot analysis.

Antibody	Dilution	Catalog#
Beta Actin	1:1000	ab8226
TTN (Titin)	1:1000	ab284860
MURF1 (TRIM63)	1:2000	pa5-76695
Goat anti-Mouse IgG (H+L), HRP	1:3000	Bio-Rad 5178-2504
Donkey anti-Rabbit IgG (H+L), HRP	1:3000	Invitrogen A16023

Western Blot

Protein isolation from rotator cuff tissue was processed using RIPA buffer with protease inhibitor and mechanically homogenized in 2.0 mL microcentrifuge Eppendorf tubes. Cells were washed twice with cold 1x PBS, RIPA buffer with protease inhibitor was added for 10 minutes at 4°C on a shaker, and then cell lysate was transferred into 2.0 mL microcentrifuge Eppendorf tubes. Homogenized tissue samples and cell lysate were centrifuged at 12,000 rpm for 15 minutes at 4°C. Protein concentration estimation was determined using Bradford Assay and the BSA standard curve. Protein was diluted in 4× Laemmli Sample Buffer (Bio-Rad #1610747) with a reducing agent, 2.5% beta-mercaptoethanol, according to concentration calculations for 20-30µg of protein. Proteins were separated using SDS-PAGE with 10-well Mini PROTEAN TGX Pre-cast Gels (4%-15%) and Precision Plus Protein Standard in Dual Color (Bio-Rad # 1610374) followed by wet transfer to PVDF membrane. After transfer, total protein was checked with Ponceau S Solution (P7170), imaged, and then washed using 1× Tris-Buffered Saline with 0.1% Tween 20 (TBS-T). Once the pink color was completely washed out, blocking buffer (5% non-fat milk in TBST) was added and incubated for 1 hour at room temperature. Primary antibodies (Table 3) were prepared in a blocking buffer and incubated overnight at 4°C. Primary antibodies were re-collected and the PVDF membrane was washed 3 times with TBS-T for 5 minutes each. Then, the secondary antibody (Table 2) was incubated for 45 minutes at room temperature. Chemiluminescence was detected using Pierce ECL Western Blotting Substrate (32106) by adding equal amounts of reagent 1 and reagent 2 to the PVDF membrane right before scanning on the Bio-Rad ChemiDoc™ MP Imaging System.

Statistical Analysis

Data is presented as the mean ± SEM. Data were analyzed using GraphPad Prism 9. For IHC, RT-qPCR, and Western blots, the comparison between two groups for the expression of the protein or gene of interest was performed using a two-tailed Student's t-test. The comparison between more than two groups for the expression of the protein and transcripts of interest was performed using One-way ANOVA with Bonferroni's posthoc test. A probability (p) value < 0.05 was accepted as statistically significant. *p <0.05, **p<0.01, ***p <0.001 and ****p <0.0001.

Results

Hypercholesterolemia is associated with muscle atrophy, inflammation, and fatty infiltration in Rotator Cuff Muscles

Hematoxylin and eosin (H&E) staining of normal skeletal muscle tissue depicted distinct muscle fiber bundle morphology with minimal instances of fatty infiltration and minimal leukocyte infiltration (Figure 1A). H&E staining of hypercholesterolemic skeletal muscle tissue revealed an altered muscle morphology compared to normal tissues. There was increased fatty infiltration in between muscle bundles and in between muscle fibers, which can be detected by the floating, purple-stained nuclei (eccentric nucleus) and pink-stained cytoplasm characterizing adipocyte. The presence of mono-lobed nuclei macrophages along the fascia of muscle fibers suggest the presence of inflammation. The most obvious difference in morphology is the disorganization of muscle fibers and decreased myofibril size in the hypercholesterolemic tissue, which is stained in pink (Figure 1B) compared to normal tissues (Figure 1A). The presence of leukocyte, adipocyte, and myofibril atrophy in hypercholesterolemic tissue prompted further immunohistochemical and transcriptional investigation of pro-inflammatory cytokines and chemokines including interleukin (IL)-6, tumor necrosis factor (TNF)-α, IL-1β, monocyte chemoattractant protein (MCP)-1, macrophage markers (CD68, CD86, CD206, and CD163), adipocyte cytokines (adiponectin and leptin), and atrophy-specific markers including myoblast determination protein (MYOD)1, Forkhead box O3 (FOXO3), Tripartite Motif Containing 63 (TRIM63/MuRF1), and titin.

Masson's Trichrome staining revealed the difference in skeletal muscle fiber size between normal and hypercholesterolemic supraspinatus muscle. The fiber size was like the atrophy observed in the H&E staining. Masson's Trichrome stain of normal supraspinatus muscle indicates uniform muscle fiber bundles and minimal sites of fatty infiltration along the fascia, which is stained in blue (Figure 1C). The most notable feature of hypercholesterolemic supraspinatus muscle was the intense blue staining of collagen in between the muscle bundle fascia, apparitions of adipocytes entangled in the collagen fibers (indicated by the black boxes in Figure 1D), and how collagen penetrates through individual muscle fibers, indicating possible sites of fibrosis. This result of increased collagen staining in hypercholesterolemic supraspinatus muscle prompted further investigation in the immunohistochemistry of collagen-I and collagen-III.

Hoangvi Le, et al., J Ortho Sports Med 2024
DOI:10.26502/josm.511500161

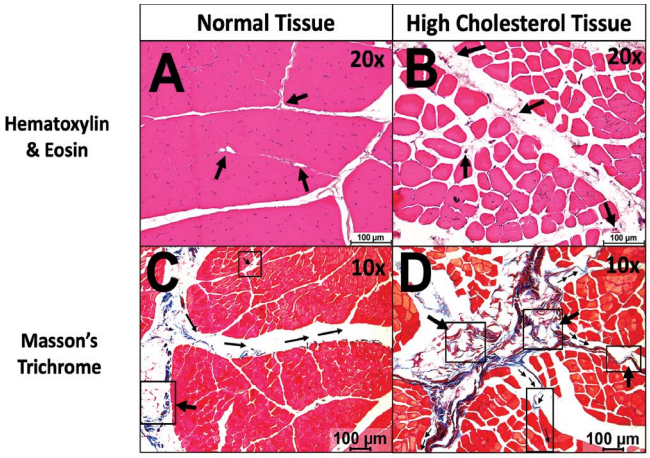

Figure 1: Hematoxylin & Eosin (A and B) and Masson's Trichrome (C and D) staining of hypercholesterolemic Yucatan microswine and control miniswine supraspinatus. Panel A shows minimal fatty infiltration in normal tissue compared to panel B, which shows more leukocyte and fatty infiltration, as well as muscle atrophy, in high cholesterol tissue, as shown in panel B. Panel C, normal tissue, shows light density of blue-stained collagen (fascia) with apparitions of adipocytes, indicated by their pink-stained cytoplasm and black nuclei, indicated in the box. Arrows show the direction of blue-stained fascia. Panel D, high cholesterol tissue, shows very dense, blue-stained collagen (fibrosis) with many apparitions of adipocytes, as indicated in the boxes. Additionally, variations in muscle fiber size indicate atrophy. 20x magnification was used in panels A and B. 10x magnification was used in panels C and D. These images are representative of 7 microswine in each group.

Hypercholesterolemia is associated with altered collagen content

Chronic inflammatory reactions induced by tissue injury can ultimately result in collagen reorganization and fibrosis. Excessive deposition of extracellular matrix components, including collagen, causes fibrosis, which leads to tissue overgrowth, hardening, and scarring [47]. To further support the finding of increased collagen staining in supraspinatus muscle with Masson's Trichrome, immunohistochemistry staining of collagen I (COL 1) and collagen III (COL 3) was done. is the results revealed a positive expression of low-density lipoprotein receptor (LDLR), COL 1, and COL 3 in the fascia (Figure 2). Upon analyzing both tissue groups, it was observed that the hypercholesterolemic tissue exhibited a significantly higher average stained intensity of pro-fibrotic collagen-III, compared to the normal tissue (Figure 2G). Although COL 1 staining showed an increase, it was not statistically significant. Notably, increased LDLR expression in the hypercholesterolemic tissue compared to normal tissues confirmed hypercholesterolemic condition [48]. These results are consistent with previous findings from other studies [49-52].

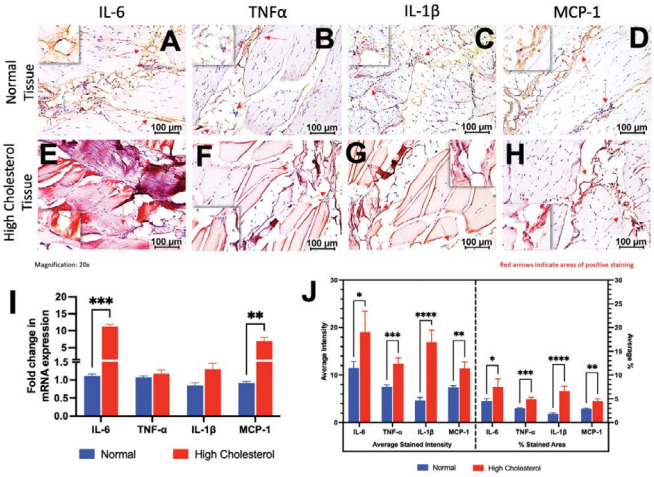

Figure 2: IHC staining of LDL receptor (LDLR), Collagen-I (COL-1), and Collagen-III (COL-3) in hypercholesterolemic supraspinatus muscle compared to normal supraspinatus muscle. Immunohistochemistry (IHC) staining of LDLR, COL-1, and COL-3 in normal (A–C) and high cholesterol tissue (D–F). (G) Average stained intensity and percent-stained area analysis of IHC staining. Red staining in panels A and D was accomplished by a 3-amino-9-ethylcarbazole (AEC) substrate kit, whereas brown staining in panels B–C and E–F was accomplished by a 3, 3'-diaminobenzidine (DAB) substrate kit. The data are presented as mean ± SEM (n = 7 in each group). **p<0.01 and ***p<0.001.

Hypercholesterolemia is associated with inflammation in the Rotator Cuff Muscle

The dysregulation of pro-inflammatory cytokine production has been implicated in the pathogenesis of various chronic inflammatory diseases including RCI [53,54]. To investigate this, immunohistochemistry of cytokines and chemokine of the pro-inflammatory response, IL-6, TNF-α, IL-1β, and MCP-1, were tested. IHC staining revealed a significantly increased immunopositivity for pro-inflammatory cytokines and MCP-1 in the skeletal muscle fascia of the hypercholesterolemic tissues compared to the control tissues (Figure 3 panels A-H and I). The RT-PCR studies revealed significantly increased transcript levels of IL-6 and MCP-1 in hypercholesterolemic tissues compared to control muscle tissue (Figure 3I). The IHC and RT-PCR results support the findings of the presence of persistent inflammation in the hypercholesterolemic tissues. The main question that remains unanswered is the source of these pro-inflammatory cytokines. However, based on the current results, it is highly likely that macrophages [55] or adipocytes [56] are the major sources of these cytokines. Given that the hypercholesterolemic microswine were exposed to a high-cholesterol diet for one year before sacrifice, the phenotype of macrophages and adipocytes in this model may differ from their typical characterization under normal conditions. To investigate this possibility, immunohistochemistry and gene expression analyses were performed to confirm the source of pro-inflammatory cytokines.

Hoangvi Le, et al., J Ortho Sports Med 2024
DOI:10.26502/josm.511500161

Hypercholesterolemia is associated with increased macrophage infiltration in Rotator Cuff Muscles

Macrophages have been known to play a role in the perpetuation of chronic inflammation in hypercholesterolemia [57]. In response to pro-inflammatory cytokines, macrophages produce additional cytokines, which attract more immune cells to the site of inflammation [55,58]. This leads to a vicious cycle of immune activation and inflammation. IHC for macrophages (CD68+), pro-inflammatory M1 macrophages (CD86+), and anti-inflammatory M2 macrophages (CD206+ for M2a and CD163+ for M2b) showed that macrophages are predominantly localized in the skeletal muscle fascia, where pro-inflammatory cytokines were also observed (Figure 4 A-H). IHC image analysis revealed a statistically significantly decreased macrophages (CD68+) and M2 macrophages (CD206+) while an increase in M1 macrophages (CD86+) (Figure 4 panel J) in hypercholesterolemic swine compared to control swine. These findings were supported by the average stained intensity and average stained percent area (Figure 4 panel J). To our surprise the mRNA transcript of CD68, CD86, and CD 206 with PCR (Figure 4 panel I) in the control and hypercholesterolemic tissues were not consistent with IHC findings. The mRNA transcripts showed increased CD68 and CD206 while decreased CD86 and CD163 in hypercholesterolemic tissues compared to normal tissues. The mRNA transcripts suggest the presence of inflammation (increased CD68) and the immune response of the body (increased CD206) in the hypercholesterolemic group. However, decreased mRNA transcript for M1 macrophages in the presence of inflammation and increased CD86 protein expression on IHC is inconsistent and this may be due to transcriptional or post-transcriptional regulation. Another reason may be the duration of hypercholesterolemic diet, and the surgery and treatment given to these swine for other project conducted on these swine [59].

Hypercholesterolemia upregulates leptin expression in rotator cuff muscles.

In hypercholesterolemic conditions, increased secretion of pro-inflammatory adipokine leptin and decreased secretion of anti-inflammatory adipokine adiponectin from hypertrophied and hyperplastic adipocytes contributes to persistent low-grade inflammation [60,61]. Adipocytes also promote the recruitment of macrophages further amplifing inflammation through the production of pro-inflammatory cytokines. To examine the primary sites of expression for adiponectin (ADIPOQ) and leptin (LEP), IHC was performed, and the results revealed immunopositivity for adiponectin and leptin in the skeletal muscle fascia where adipocyte apparitions were detected through H&E staining (Figure 5 A-D). Upon analyzing the average stained intensity and percent average stained area, we checked mRNA expression of Leptin-lean as well as leptin-obese using different primers because

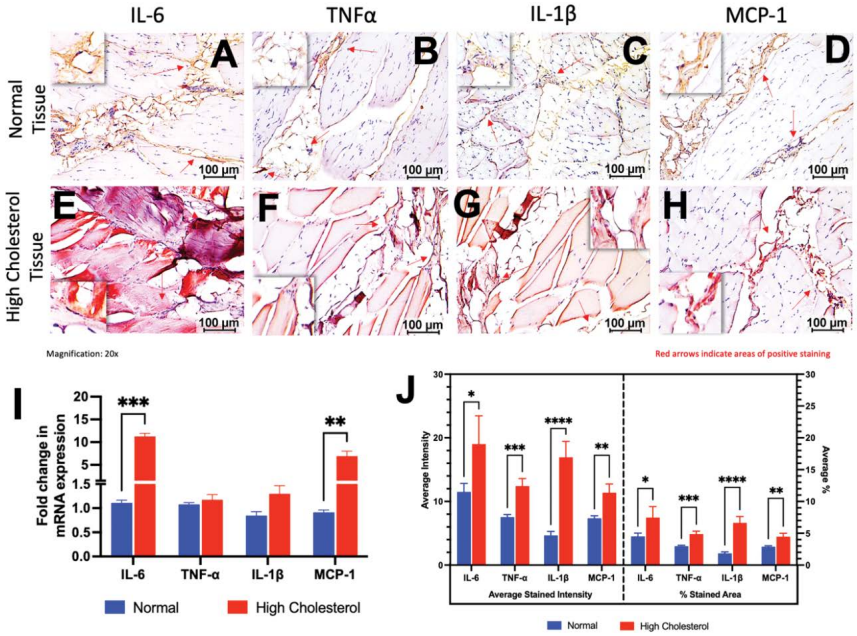

Figure 3: Pro-inflammatory cytokines transcriptional and semi-quantitative protein expression in hypercholesterolemic supraspinatus muscle compared to normal supraspinatus muscle. Immunohistochemistry (IHC) staining of IL-6, TNF-α, IL-1β, and MCP-1 in normal (A–D) and high cholesterol tissue (E–H). (I) Fold change in mRNA expression between normal and hypercholesterolemic tissue. (J) Average stained intensity (left side) and percent-stained area (%; right side) analysis of IHC staining. Brown staining in panels A–D was accomplished by the DAB substrate kit, whereas red staining in panels E–H was accomplished by the AEC substrate kit. Student's t-test was used for statistical analyses. The data are presented as mean ± SEM (n = 7 in each group). *p<0.05, **p<0.01, ***p<0.001, ****p<0.0001. The images are representative of all swine involved in this study.

Hoangvi Le, et al., J Ortho Sports Med 2024
DOI:10.26502/josm.511500161

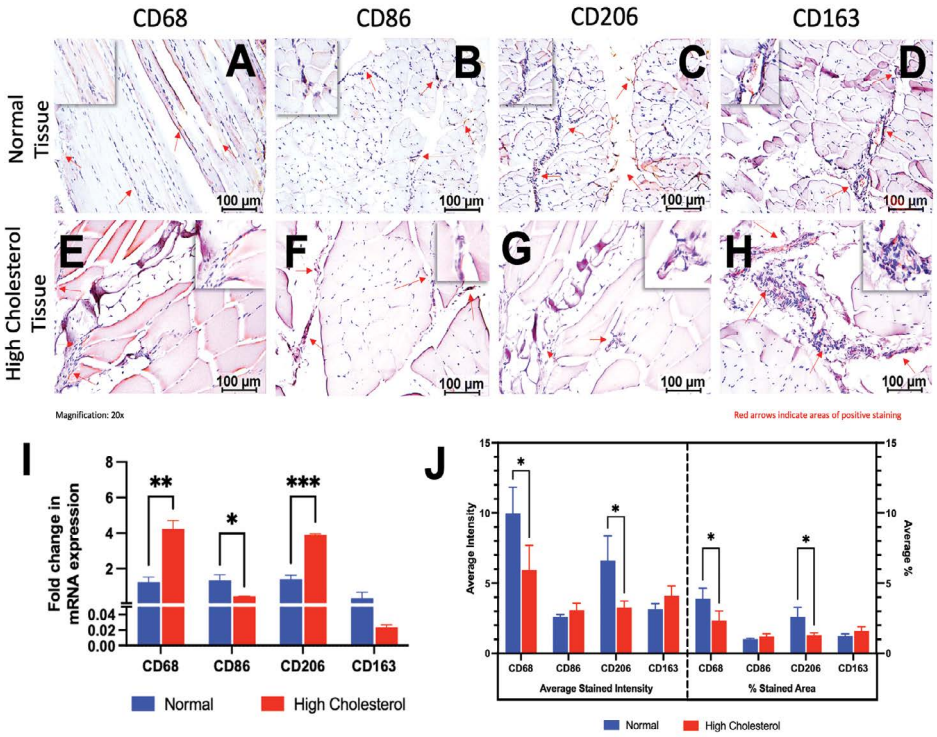

Figure 4: Immunostaining and PCR analysis of macrophages in hypercholesterolemic supraspinatus muscles compared to control supraspinatus muscle. (A–H) Immunohistochemistry (IHC) staining of CD68, CD86, CD206, and CD163. (I) Fold change in mRNA expression between normal and hypercholesterolemic tissue. (J) Average stained intensity and percent-stained area analysis of IHC staining. Brown staining in panels A–C was accomplished by the DAB substrate kit, whereas red staining in panels D–H was accomplished by the AEC substrate kit. The data are presented as mean ± SEM (n = 7 in each group). *p<0.05, **p<0.01, ***p<0.001. The images are representative of all swine involved in this study.

leptin levels may cause weight loss and the swine were on different types of diet (normal vs hypercholesterolemic). it was observed that both adiponectin and leptin expression were significantly increased (Figure 5F). These findings were validated by the significantly increased gene expression levels of both *ADIPOQ* and *LEP* (Figure 5E) in hyperlipidemic muscle tissues.

Hypercholesterolemia upregulates atrophy-specific transcription factors.

Myoblast determination protein 1 (MYOD1) and Forkhead box O3 (FOXO3) have been shown to co-express in vitro and depend on each other for myotube stability [62]. To examine the expression of FOXO3 and MYOD1 in tissues, IHC was performed. However, due to the unavailability of swine specific MYOD1 antibodies, MYOG was used instead as both are classified under myogenic regulatory factors (MRFs) [63]. Interestingly, FOXO3 and MYOG were positively stained in skeletal muscle fascia in the histological location where pro-inflammatory cytokines were detected (Figure 6 A–D). Both FOXO3 and MYOG exhibited a significant increase in expression, as determined by the analysis of the percent-stained area and average stained intensity (Figure 6F). These findings were validated by the significantly increased gene expression levels of *MYOD1* and *FOXO3* (Figure 6E). In summary, the observed increase in these factors suggests a mechanism adapted by the body to maintain decreasing muscle mass in response to hypercholesterolemia-associated inflammation and atrophy. However, the concern is why in the presence of increased expression of these factors, the muscle mass is atrophied on H and E staining. This may be either due to persistent inflammation degrading muscle proteins and regeneration may take longer time (the swine were sacrificed after 1 year) and the continued hypercholesterolemic diet. We next analyzed the muscle proteins in both groups.

Hypercholesterolemia upregulates atrophy-specific marker TRIM63 in rotator cuff muscles.

The E3 ubiquitin ligase MuRF1/TRIM63 plays an important role in skeletal muscle atrophy [64]. Positive TRIM63 staining was observed in the skeletal muscle fascia of hypercholesterolemic tissues (Figure 7C) [65,66]. Increased MURF1 expression is associated with titin degradation [67]. IHC revealed immunopositivity for titin in the expected general area of skeletal muscle (Figure 7 B & D) and titin expression was significantly decreased in hypercholesterolemic tissues (Figure 7E). RT-qPCR and Western blot analysis of TRIM63 and titin (*TTN*) supported the

Hoangvi Le, et al., J Ortho Sports Med 2024
DOI:10.26502/josm.511500161

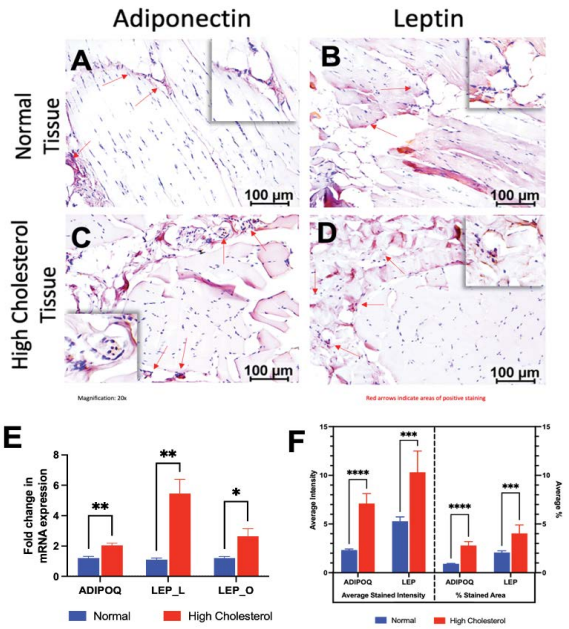

Figure 5: Adipocyte cytokines transcriptional and semi-quantitative protein expression in hypercholesterolemic supraspinatus muscle compared to normal supraspinatus muscle. (A–D) Immunohistochemistry (IHC) staining of Adiponectin (ADIPOQ) and Leptin (LEP). (E) Fold change in mRNA expression between normal and hypercholesterolemic tissue (ADIPOQ = Adiponectin; LEP_L = Leptin "Lean"; LEP_O = Leptin "Obese"). (F) Average stained intensity and percent-stained area analysis of IHC staining. Brown staining in panels A–D was accomplished by the DAB substrate kit. The data are presented as mean ± SEM (n = 7 in each group). *p<0.05, **p<0.01, ***p<0.001, ****p<0.0001. The images are representative of all swine involved in this study.

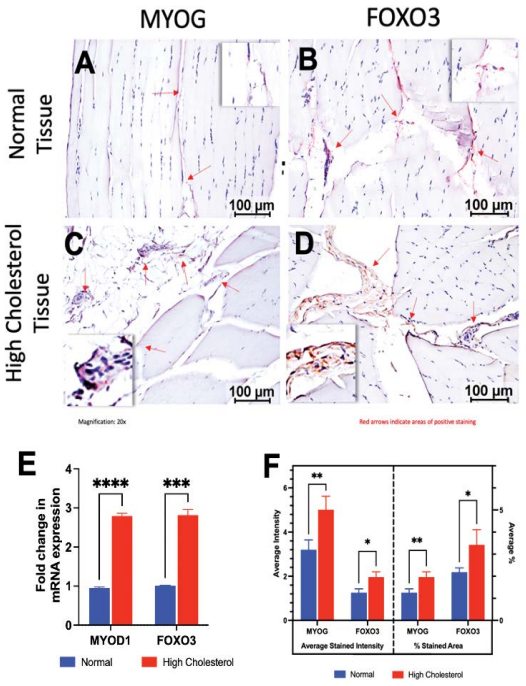

Figure 6: Atrophy-specific transcription factors gene expression and semi-quantitative protein expression in hypercholesterolemic supraspinatus muscle compared to normal supraspinatus muscle. (A–D) Immunohistochemistry (IHC) staining of MYOG and Leptin. (E) Fold change in mRNA expression of MYOD1 and FOXO3 between normal and hypercholesterolemic tissue. (F) Average stained intensity and percent-stained area analysis of IHC staining. Red staining in panels A–D was accomplished by the AEC substrate kit. The data are presented as mean ± SEM (n = 7 in each group). *p<0.05, **p<0.01, ***p<0.001, ****p<0.0001. The images are representative of all swine involved in this study.

results of IHC and PCR (Figure 7 F–H). Overall, these results showed a significant increase in both the gene and protein expression of TRIM63, and its association with decreased titin gene and protein expression suggests an upregulation of muscle atrophy in hypercholesterolemic tissues.

Discussion

The results of this study revealed that hypercholesterolemia is associated with increased fatty infiltration, leukocyte infiltration, decrease in muscle mass (atrophy), expression of pro-inflammatory cytokines and chemokines, and altered collagens. The findings suggest that chronic low-grade inflammation could lead to decreased muscle mass due to degradation of muscle protein titin. Chronic inflammation is known to cause fibrosis by promoting the deposition of extracellular matrix (ECM) components, particularly collagen [68]. In our study, we observed increased levels of pro-inflammatory cytokines and chemokines, macrophages, and adipokines in hypercholesterolemic tissue. This suggests an association of hypercholesterolemia with persistent inflammation and decreased muscle mass. Pro-inflammatory cytokines can promote the activation and differentiation of fibroblasts into myofibroblasts, which are responsible for the deposition of ECM components. Interestingly, we also observed an increase in LDLR levels in the experimental tissue, confirming the hypercholesterolemic condition. This finding may have implications for the development of fibrosis, as high levels of LDL have been shown to promote fibrosis in various tissues, including the liver and heart [68]. LDL can stimulate the production of transforming growth factor-beta (TGF-β), a key mediator of fibrosis, and promote the activation of myofibroblasts [70]. A key finding of this study was adipocytes as the source of pro-inflammatory cytokines in hypercholesterolemic rotator cuff muscle, further investigations are needed to confirm this hypothesis. The inconsistent results for the protein and gene expression for macrophages, M1 (CD86+), and M2 macrophages (CD206+ and CD163+), transcriptional and post-translational modification may have contributed to this and the role of transcription factors and microRNAs (miRNAs), both regulating the gene expression, in the presence of hypercholesterolemia should be investigated [71,72].

Hoangvi Le, et al., J Ortho Sports Med 2024
DOI:10.26502/josm.511500161

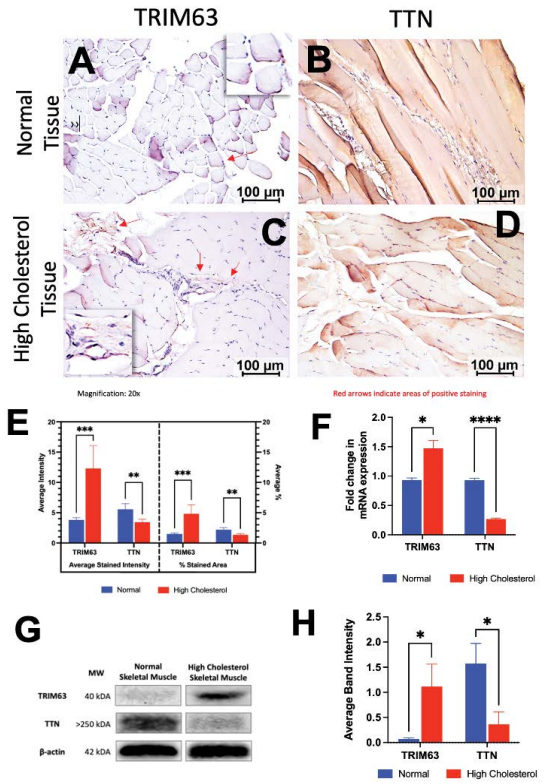

Figure 7: TRIM63 and titin gene expression and protein expression in hypercholesterolemic supraspinatus muscle compared to normal supraspinatus muscle. (A–D) Immunohistochemistry (IHC) staining of TRIM63 and TTN. (E) Average stained intensity and percent-stained area analysis of IHC staining. (F) Fold change in mRNA expression between normal and hypercholesterolemic tissue. (G) Western blot of TRIM63 and titin in normal and high cholesterol skeletal muscle; Beta-actin is the loading control. (H) Average band intensity of TRIM63 and titin protein. Brown staining was accomplished by DAB. The data are presented as mean ± SEM (n = 7 in each group). *p<0.05, **p<0.01, ***p<0.001, ****p<0.0001. The images are representative of all swine involved in this study.

Skeletal muscle and adipocytes depend on each other to coordinate metabolism and tissue regeneration [73,74]. Fatty infiltration of skeletal muscle is characterized by dysfunctional leptin signaling, loss of muscle strength, reduced insulin sensitivity, and increased mortality among the elderly [75,76]. Intramuscular fatty infiltration, typically diagnosed using imaging techniques such as magnetic resonance imaging (MRI) or computed tomography (CT) scans, refers to the accumulation of fat or adipose tissue within the muscle fibers of skeletal muscle. It is associated with several metabolic disorders, including insulin resistance, type 2 diabetes, and obesity [77]. It is also commonly seen in older adults and individuals with sedentary lifestyles. The accumulation of intramuscular fat can impair muscle function and reduce muscle strength and endurance [78] by increasing the recruitment of inflammatory macrophages and proinflammatory cytokine secretion. Fatty infiltration and macrophage infiltration of muscle tissue can also occur in normal-weight individuals with metabolic disorders [55]. The presence of adipocyte infiltration in the muscle and the presence of immune cells and cytokines in hypercholesterolemic tissues support the notion to investigate the association of hypercholesterolemia and muscle atrophy and the underlying mechanisms. Age-related metabolic alterations may affect how nutritional intake impacts endocrine functions, muscle mass homeostasis, and lipid profile [22]. Aging impacts muscle mass through sarcopenia and chronic inflammation [18,56].

Hypercholesterolemia is strongly associated with adipose tissue accumulation and adipocyte hypertrophy in response to the increased need to store excessive cholesterol and other lipids. However, adipocytes become metabolically dysfunctional when their lipid storage reaches abnormally excessive levels and consequently triggers the inflammatory response [79]. Hypercholesterolemia is often characterized by a chronic inflammatory response to LDL-cholesterol dominated by macrophages and foam cells [80]. Lipotoxicity can trigger inflammation and tissue damage as pro-inflammatory cytokines including IL-1, IL-6, TNF-α, and adipokines like leptins are released from resident and infiltrated macrophages and adipocytes [81]. Chronic inflammation can disrupt proteins in the skeletal muscle fiber triggering atrophy [82]. Chronic inflammation in skeletal muscle is dependent on macrophage kinetics and disturbance in cell signaling can lead to muscle fiber degeneration [83]. In chronic inflammation, both M1 and M2 macrophages increase and compete for arginine metabolism as arginine is a shared substrate for iNOS and arginase. However, M2c macrophages reduce the effects of cytokines secreted by M1 macrophages, leading to a shift in metabolism from iNOS to arginase, resulting in a pro-fibrotic environment. M2 macrophages also increase myogenic factors to promote regeneration in injured skeletal muscle [84]. An increase in macrophage population, M2a macrophages, and M2c macrophages in hypercholesterolemic tissues in this study suggest the response of the body to promote regeneration, however, inconsistency between gene and protein expression warrant investigation.

Mitochondrial function and mitochondrial DNA (mtDNA) can also be another relevant target in microgravity-mediated muscle atrophy caused by oxidative stress, DNA damage, and inflammation [85,86]. Reactive oxygen species (ROS) can activate NF-κB pathways and subsequent release of cytokines like TNF-α, as well as damaging the sarcolemma and contractile proteins, exacerbating muscle dysfunction in dystrophic muscle cells [87]. The findings of this study with increased fatty infiltration, macrophage recruitment, and expression of inflammatory cytokines in hyperlipidemic muscle tissues suggest a correlation of hypercholesterolemia

Hoangvi Le, et al., J Ortho Sports Med 2024
DOI:10.26502/josm.511500161

with reduced muscle mass.

Inflammation-induced striated muscle atrophy has been observed in the dysregulation of muscle fibers such as actin, myosin, and titin [88-90]. Actin fragments were generated by caspase-3 and further degraded by a ubiquitin-proteasome [91]. Muscle-specific E3 ubiquitin-ligase, TRIM63, has been shown to degrade myosin light chains 1 and 2, myosin heavy chains, and myosin-binding protein C [92]. FOXO3 is a recognized transcription factor that triggers ubiquitin ligases (TRIM63 and Atrogin-1) which induce skeletal muscle atrophy [93]. A recent transcriptome study demonstrated that transfecting myotubes with an active mutant of FOXO3, FOXO3a, decreased average myotube diameter by 27.5%, demonstrating the important role of FOXO3 in regulating muscle atrophy [94,95]. TRIM63 was hypothesized to regulate gene expression in skeletal muscle through ubiquitination events, allowing it to coordinate with myogenic regulatory factors and control gene activity at the transcriptional level. Expression of TRIM63 and myogenic factors, MYOD1 and MYOG, were shown to increase with denervation, which results in muscle atrophy [96]. Increased expression of E3 ubiquitin ligases (TRIM62, TRIM63, and Atrogin-1) was associated with inflammation and skeletal muscle atrophy. Inhibition of pro-inflammatory cytokine, IL-6, was observed when knockout TRIM62 C2C12 myotubes [97]. An animal study has shown that there is an inverse correlation between the gene expression of titin (TTN) and TRIM63 in skeletal muscle atrophy [98] (Figure 1). While full-length TTN-KO in mice resulted in embryonic lethality, knockout of Z-disc-anchored TTN successfully demonstrated skeletal muscle atrophy in mice [99]. TRIM63 has also been observed in titin degradation in cardiomyopathies [100].

The results of immunohistochemical staining and gene expression analysis revealing upregulation of skeletal muscle atrophy-specific transcription factors in the presence of persistent inflammation suggest that inflammation may be a crucial factor inducing muscle atrophy. Specifically, positive staining for FOXO3 and MYOG was observed in the skeletal muscle fascia of hypercholesterolemic tissue, and gene expression levels of MYOD1 and FOXO3 were increased. This synergy between FOXO3 and MYOD1 was also observed in another animal study [62]. Additionally, these findings support the theory that chronic inflammation drives the upregulation of skeletal muscle atrophy through FOXO3 [101-103]. Furthermore, this study found that TRIM63 was significantly upregulated in hypercholesterolemia tissue, indicating an upregulation of muscle atrophy; while TTN gene and protein expression were significantly decreased, indicating a decrease in muscle integrity and function. These results further support TRIM63 as a recognized marker for muscle atrophy in human, rodent, and swine models [104]. Additionally, our results of decreased titin support the findings of previous research that have also indicated titin loss as an indication of weak skeletal muscle integrity and dysfunction [99,105]. Overall, these results suggest that TRIM63 and TTN may have important roles in the development of muscle atrophy and loss of muscle function in the context of chronic inflammation observed in hypercholesterolemia. Further research is needed to understand the underlying mechanisms and develop potential therapeutic strategies to prevent or treat muscle atrophy in chronic inflammatory conditions.

Overall, the results of this study suggest that hypercholesterolemia in muscle can cause chronic inflammation by adipocyte hypertrophy, thus increased secretion of adipokine, leptin, which signals a pro-inflammatory vascular response and recruit immune cells such as monocytes, neutrophils, and dendritic cells to infiltrate the muscle tissue. Monocytes that infiltrate the inflamed muscle tissue are transformed into macrophages (M1 or M2) in the presence of pro- and anti-inflammatory cytokines. Mixed crosstalk signaling from macrophages and cytokines can lead to upregulation of transcription factors, MYOD1 and FOXO3, which will signal for increased TRIM63 expression and ultimately lead to titin degradation in fast-twitch skeletal muscle fibers.

Conclusion

The results of this study have shed light on the negative impact of hypercholesterolemia on skeletal muscle tissue, specifically the rotator cuff muscle. The findings indicate a cross-talk between inflammation-MYOD1/FOXO3/TRIM63-titin degradation in the presence of hypercholesterolemia in the skeletal muscles. The results have contributed to the understanding of how hypercholesterolemia affects skeletal muscle tissue. The findings of this study may have implications for the development of therapeutic strategies to prevent or treat muscle atrophy in chronic inflammatory conditions, such as hypercholesterolemia in the general population, cancer patients, and astronauts- the translational aspect of this study. Future studies should aim to investigate the underlying molecular mechanisms of how LDL causes skeletal muscle atrophy and explore potential therapeutic targets to prevent or treat this condition.

Future Perspectives

Further research in mimicking the effects of hypercholesterolemia in C2C12 myotubes would provide great insight into the direct mechanism between LDL and markers of muscle atrophy. One potential area of focus could be the role of titin degradation in these processes. Preventing titin degradation may have significant therapeutic implications, either by preventing the onset of muscle atrophy or by enhancing muscle repair following injury. However, more research will be necessary to fully explore this hypothesis and its potential clinical applications.

Additionally, investigating the roles of ApoB and LDLR in regulating the FOXO3/TRIM63/Titin axis, as well as the involvement of transcription factors and miRNAs, may provide further insight into the molecular pathways involved in muscle atrophy and related conditions. Methods like FISH (fluorescent in situ hybridization) can confirm co-expression between FOXO3, TRIM63, and Titin in FFPE rotator cuff tissues using kits that offer multiplex fluorescence, such as ACD RNAscope™ Multiplex Fluorescent Detection Kit. To take this one step further, NanoString can use these fluorescent morphology probes to capture regions of interest (ROIs) to sequence by subjecting the tissue to an additional hybridization step. Another method developed by 10× Genomics uses in situ polyadenylation to reveal coding and noncoding RNAs. The results from transcriptome spatial sequencing would reveal precisely which genes are upregulated during muscle atrophy. However, the success of spatial sequencing relies on fresh tissue due to the instability of mRNA. Overall, continued investigation into the complex signaling between cytokines and cellular degradation pathways will be critical for developing new treatments and preventative strategies for muscle atrophy and related conditions.

Limitations of the Study

This study revealed a significant correlation between hypercholesterolemia-induced chronic inflammation with muscle atrophy. However, there are a few limitations. Firstly, the use of two different breeds of Yucatan miniswine and Yucatan microswine in the in-vivo study. The use of hyperlipidemic miniswine would have contributed to the validation of our results. To address this, we did preliminary studies, and the results support that hypercholesterolemia in miniswine is also associated with decreased muscle mass and atrophy (Supplementary Figure S1, S2, S3, and S4). Second, the study did not investigate potential interventions to reduce chronic inflammation in hypercholesterolemic rotator cuff muscle tissue, which would be of great interest to future research. Additionally, the parametric statistical analyses employed assume that our data adheres to a normal distribution, however, due to the limited sample size, this could not be validated.

Author Contribution: Concept and design: HL, VR, and DKA; Conduct of the Experiments: HL, VR; Analysis and interpretation of the data: HL, VR; Drafting the article: HL and VR; Revising and editing the manuscript: VR and DKA; Final approval of the article: HL, VR, DKA.

Funding: The research work of DKA is supported by the R01 HL144125 and R01 HL147662 grants from the National Institutes of Health, USA. The contents of this original research article are solely the responsibility of the authors and do not necessarily represent the official views of the National Institutes of Health.

Institutional Review Board Statement:

Not Applicable

Informed Consent Statement: All the authors have read the manuscript and consented for publication.

Acknowledgments: Not Applicable

Conflicts of Interest: All authors have read the journal's authorship agreement and policy on disclosure of potential conflicts of interest. The authors declared no conflict of interest. No writing assistance was utilized in the production of this manuscript.

References

1. Martin PK, Bowman R, Bachle S, et al. IG-21-025: NASA's Development of Next-Generation Spacesuits. National Aeronautics and Space Administration (NASA) (2021).
2. Anderson AP, Newman DJ, Welsch RE. Statistical Evaluation of Causal Factors Associated with Astronaut Shoulder Injury in Space Suits. Aerosp Med Hum Perform 86 (2015): 606-613.
3. Hilbert AM. Human-spacesuit interaction. Massachusetts Institute of Technology (2015).
4. Laughlin MS, Murray JD, Foy M, et al. Shoulder Injury Incidence Rates In Nasa Astronauts (2014).
5. Murray JD, Laughlin MS, Foy M, et al. Rate of Shoulder Surgery Among Nasa Astronauts (2014).
6. Abboud JA, Kim JS. The effect of hypercholesterolemia on rotator cuff disease. Clin Orthop Relat Res 468 (2010): 1493-1497.
7. Kumar DV, Shetty M, Shetty S, et al. Association between dyslipidemia and rotator cuff tear–A study. Biomedicine 43 (2023): 1838-1843.
8. Yang Y, Qu J. The effects of hyperlipidemia on rotator cuff diseases: a systematic review. J Orthop Surg Res 13 (2018): 204.
9. Qian Y, Huang H, Wan R, et al. Progress in studying the impact of hyperlipidemia and statins on rotator cuff injury and repair. Front Public Health 11 (2023): 1279118.
10. Gatto AP, Hu DA, Feeley BT, et al. Dyslipidemia is associated with risk for rotator cuff repair failure: a systematic review and meta-analysis. JSES Reviews, Reports, and Techniques 2 (2022): 302-309.
11. Chen K, Gao P, Fang X, et al. Causal relationship between lipid profile and muscle atrophy: A bi-directional Mendelian randomization study. Animal Model Exp Med (2023).

12. Sellers SL, Milad N, White Z, et al. Increased nonHDL cholesterol levels cause muscle wasting and ambulatory dysfunction in the mouse model of LGMD2B. J Lipid Res 59 (2018): 261-272.

13. Charvat JM, Leonard D, Barlow CE, et al. Long-term Cardiovascular Risk in Astronauts: Comparing NASA Mission Astronauts with a Healthy Cohort From the Cooper Center Longitudinal Study. Mayo Clin Proc 97 (2022): 1237-1246.

14. Le H, Rai V, Agrawal DK. Cholesterol: An Important Determinant of Muscle Atrophy in Astronauts. J Biotechnol Biomed 6 (2023): 67-79.

15. Leach CS, Johnson PC, Krauhs JM, et al. Cholesterol in serum lipoprotein fractions after spaceflight. Aviat Space Environ Med 59 (1988): 1034-1037.

16. Schiaffino S, Reggiani C, Akimoto T, et al. Molecular Mechanisms of Skeletal Muscle Hypertrophy. J Neuromuscul Dis 8 (2021): 169-183.

17. Schiaffino S, Dyar KA, Ciciliot S, et al. Mechanisms regulating skeletal muscle growth and atrophy. The FEBS Journal 280 (2013): 4294-4314.

18. Zhang X, Xu D, Chen M, et al. Impacts of Selected Dietary Nutrient Intakes on Skeletal Muscle Insulin Sensitivity and Applications to Early Prevention of Type 2 Diabetes. Adv Nutr 12 (2021): 1305-1316.

19. Ahmed S, Singh D, Khattab S, et al. The Effects of Diet on the Proportion of Intramuscular Fat in Human Muscle: A Systematic Review and Meta-analysis. Front Nutr 5 (2018).

20. Fanzani A, Conraads VM, Penna F, et al. Molecular and cellular mechanisms of skeletal muscle atrophy: an update. J Cachexia Sarcopenia Muscle 3 (2012): 163-179.

21. Flück M, Hoppeler H. Molecular basis of skeletal muscle plasticity--from gene to form and function. Rev Physiol Biochem Pharmacol 146 (2003): 159-216.

22. Snijders T, Nederveen JP, McKay BR, et al. Satellite cells in human skeletal muscle plasticity. Frontiers in Physiology 6 (2015).

23. Hoppeler H, Baum O, Lurman G, et al. Molecular mechanisms of muscle plasticity with exercise. Compr Physiol 1 (2011): 1383-1412.

24. Kalyani RR, Corriere M, Ferrucci L. Age-related and disease-related muscle loss: the effect of diabetes, obesity, and other diseases. Lancet Diabetes Endocrinol 2 (2014): 819-829.

25. Lee TV, Lee CW, Chen VCW, et al. The effects of hindlimb unloading versus dietary cholesterol and resistance training on rat skeletal muscle responses. Lipids in Health and Disease 18 (2019): 3.

26. Barrientos G, Llanos P, Hidalgo J, et al. Cholesterol removal from adult skeletal muscle impairs excitation–contraction coupling and aging reduces caveolin-3 and alters the expression of other triadic proteins. Frontiers in Physiology (2015).

27. Possidonio AC, Miranda M, Gregoracci GB, et al. Cholesterol depletion induces transcriptional changes during skeletal muscle differentiation. BMC Genomics 15 (2014): 544.

28. Liu HH, Li JJ. Aging and dyslipidemia: a review of potential mechanisms. Ageing Res Rev 19 (2015): 43-52.

29. Rosada A, Kassner U, Weidemann F, et al. Hyperlipidemias in elderly patients: results from the Berlin Aging Study II (BASEII), a cross-sectional study. Lipids Health Dis 19 (2020): 92.

30. NASA. HRR - Gap - CV-203: Test countermeasures on the ISS against the spaceflight-induced changes in the cardiovascular system of importance for development of disease (2022).

31. Andrich DE, Ou Y, Melbouci L, et al. Altered Lipid Metabolism Impairs Skeletal Muscle Force in Young Rats Submitted to a Short-Term High-Fat Diet. Front Physiol 9 (2018): 1327.

32. Li YJ, Chen TH, Wu YZ, et al. Metabolic and Nutritional Issues Associated with Spinal Muscular Atrophy. Nutrients 12 (2020).

33. Deguise MO, Baranello G, Mastella C, et al. Abnormal fatty acid metabolism is a core component of spinal muscular atrophy. Ann Clin Transl Neurol 6 (2019): 1519-1532.

34. Rudrappa SS, Wilkinson DJ, Greenhaff PL, et al. Human Skeletal Muscle Disuse Atrophy: Effects on Muscle Protein Synthesis, Breakdown, and Insulin Resistance—A Qualitative Review. Frontiers in Physiology 7 (2016).

35. Czech MP, Corvera S. Signaling mechanisms that regulate glucose transport. J Biol Chem 274 (1999): 1865-1868.

36. Grice BA, Barton KJ, Covert JD, et al. Excess membrane cholesterol is an early contributing reversible aspect of skeletal muscle insulin resistance in C57BL/6NJ mice fed a Western-style high-fat diet. American Journal of Physiology-Endocrinology and Metabolism 317 (2019): E362-E373.

37. Maiti A, Daschakraborty S. How Do Urea and Trimethylamine N-Oxide Influence the Dehydration-Induced Phase Transition of a Lipid Membrane? The Journal of Physical Chemistry B 125 (2021): 10149-10165.

38. Campbell NR, Wickert W, Magner P, et al. Dehydration during fasting increases serum lipids and lipoproteins. Clin Invest Med 17 (1994): 570-576.

39. Watso JC, Farquhar WB. Hydration Status and Cardiovascular Function. Nutrients 11 (2019).

40. Cleary MA, Sitler MR, Kendrick ZV. Dehydration and symptoms of delayed-onset muscle soreness in normothermic men. J Athl Train 41 (2006): 36-45.

41. Shaheen NA, Alqahtani AA, Assiri H, et al. Public knowledge of dehydration and fluid intake practices: variation by participants' characteristics. BMC Public Health 18 (2018): 1346.

42. Biltz NK, Collins KH, Shen KC, et al. Infiltration of intramuscular adipose tissue impairs skeletal muscle contraction. J Physiol 598 (2020): 2669-2683.

43. Weinbrenner T, Züger M, Jacoby GE, et al. Lipoprotein metabolism in patients with anorexia nervosa: a case-control study investigating the mechanisms leading to hypercholesterolaemia. Br J Nutr 91 (2004): 959-969.

44. Lee JH, Lee HS, Cho AR, et al. Relationship between muscle mass index and LDL cholesterol target levels: Analysis of two studies of the Korean population. Atherosclerosis 325 (2021): 1-7.

45. Luo W, Chen J, Li L, et al. c-Myc inhibits myoblast differentiation and promotes myoblast proliferation and muscle fibre hypertrophy by regulating the expression of its target genes, miRNAs and lincRNAs. Cell Death Differ 26 (2019): 426-442.

46. Landini G, Martinelli G, Piccinini F. Colour deconvolution: stain unmixing in histological imaging. Bioinformatics 37 (2020): 1485-1487.

47. Wynn TA. Cellular and molecular mechanisms of fibrosis. J Pathol 214 (2008): 199-210.

48. Malloy SI, Altenburg MK, Knouff C, et al. Harmful effects of increased LDLR expression in mice with human APOE*4 but not APOE*3. Arterioscler Thromb Vasc Biol 24 (2004): 91-97.

49. Giovarelli M, Arnaboldi F, Zecchini S, et al. Characterisation of Progressive Skeletal Muscle Fibrosis in the Mdx Mouse Model of Duchenne Muscular Dystrophy: An In Vivo and In Vitro Study. Int J Mol Sci 23 (2022).

50. Miller NE, Weinstein DB, Carew TE, et al. Interaction between high density and low density lipoproteins uptake and degradation by cultured human fibroblasts. J Clin Invest 60 (1977): 78-88.

51. Mann CJ, Perdiguero E, Kharraz Y, et al. Aberrant repair and fibrosis development in skeletal muscle. Skeletal Muscle 1 (2011): 21.

52. Gu HM, Zhang DW. Hypercholesterolemia, low density lipoprotein receptor and proprotein convertase subtilisin/kexin-type 9. J Biomed Res 29 (2015): 356-361.

53. Abraham AC, Shah SA, Thomopoulos S. Targeting Inflammation in Rotator Cuff Tendon Degeneration and Repair. Tech Shoulder Elb Surg 18 (2017): 84-90.

54. Yazdani AN, Abdi A, Patel P, et al. Mitochondrial Biogenesis as a Therapeutic Target for Rotator Cuff Tendon Tears. J Orthop Sports Med 5 (2023): 442-449.

55. Lee CH, Choi EY. Macrophages and inflammation. Journal of Rheumatic Diseases 25 (2018): 11-18.

56. Coppack SW. Pro-inflammatory cytokines and adipose tissue. Proc Nutr Soc 60 (2001): 349-356.

57. Dib L, Koneva LA, Edsfeldt A, et al. Lipid-associated macrophages transition to an inflammatory state in human atherosclerosis increasing the risk of cerebrovascular complications. Nat Cardiovasc Res 2 (2023): 656-672.

58. Fujiwara N, Kobayashi, K. Macrophages in inflammation. Curr Drug Targets Inflamm Allergy 4 (2005): 281-286.

59. Nooti S, Rai V, Radwan MM, et al. Oxidized Low-density Lipoproteins and Lipopolysaccharides Augment Carotid Artery Plaque Vulnerability in Hypercholesterolemic Microswine. Cardiol Cardiovasc Med 7 (2023): 273-294.

60. La Cava A. Leptin in inflammation and autoimmunity. Cytokine 98 (2017): 51-58.

61. Esfahani M, Movahedian A, Baranchi M, et al. Adiponectin: an adipokine with protective features against metabolic syndrome. Iran J Basic Med Sci 18 (2015): 430-442.

62. Hu P, Geles KG, Paik JH, et al. Codependent activators direct myoblast-specific MyoD transcription. Dev Cell 15 (2008): 534-546.

63. Adhikari A, Kim W, Davie J. Myogenin is required for assembly of the transcription machinery on muscle genes during skeletal muscle differentiation. PLoS One 16 (2021): e0245618.

64. Peris-Moreno D, Taillandier D, Polge C. MuRF1/TRIM63, Master Regulator of Muscle Mass. Int J Mol Sci 21 (2020).

65. Assereto S, Piccirillo R, Baratto S, et al. The ubiquitin ligase tripartite-motif-protein 32 is induced in Duchenne muscular dystrophy. Laboratory Investigation 96 (2016): 862-871.

66. Chemello F, Wang Z, Li H, et al. Degenerative and

regenerative pathways underlying Duchenne muscular dystrophy revealed by single-nucleus RNA sequencing. Proceedings of the National Academy of Sciences 117 (2020): 29691-29701.

67. Higashikuse Y, Mittal N, Arimura T, et al. Perturbation of the titin/MURF1 signaling complex is associated with hypertrophic cardiomyopathy in a fish model and in human patients. Dis Model Mech 12 (2019).

68. Wynn TA, Ramalingam TR. Mechanisms of fibrosis: therapeutic translation for fibrotic disease. Nat Med 18 (2012): 1028-1040.

69. Watanabe S, Kumazaki S, Kusunoki K, et al. A High-Fat and High-Cholesterol Diet Induces Cardiac Fibrosis, Vascular Endothelial, and Left Ventricular Diastolic Dysfunction in SHRSP5/Dmcr Rats. J Atheroscler Thromb 25 (2018): 439-453.

70. Biernacka A, Dobaczewski M, Frangogiannis NG. TGF-β signaling in fibrosis. Growth Factors 29 (2011): 196-202.

71. Sumit J, Vrantika C, Neelam RY. Transcription Factors and MicroRNA Interplay: A New Strategy for Crop Improvement. In Transcriptional and Post-transcriptional Regulation In Eds: Kais G, Eds. IntechOpen: Rijeka (2018): 6.

72. Zhang HM, Kuang S, Xiong X, et al. Transcription factor and microRNA co-regulatory loops: important regulatory motifs in biological processes and diseases. Brief Bioinform 16 (2015): 45-58.

73. Mitchell R, Mellows B, Sheard J, et al. Secretome of adipose-derived mesenchymal stem cells promotes skeletal muscle regeneration through synergistic action of extracellular vesicle cargo and soluble proteins. Stem Cell Research & Therapy 10 (2019): 116.

74. Takada S, Sabe H, Kinugawa S. Abnormalities of Skeletal Muscle, Adipocyte Tissue, and Lipid Metabolism in Heart Failure: Practical Therapeutic Targets. Frontiers in Cardiovascular Medicine 7 (2020).

75. Hamrick MW, McGee-Lawrence ME, Frechette DM. Fatty Infiltration of Skeletal Muscle: Mechanisms and Comparisons with Bone Marrow Adiposity. Front Endocrinol (Lausanne) 7 (2016): 69.

76. Miljkovic I, Kuipers AL, Cauley JA, et al. Greater Skeletal Muscle Fat Infiltration Is Associated With Higher All-Cause and Cardiovascular Mortality in Older Men. The Journals of Gerontology: Series A 70 (2015): 1133-1140.

77. Roberts CK, Hevener AL, Barnard RJ. Metabolic syndrome and insulin resistance: underlying causes and modification by exercise training. Compr Physiol 3 (2013): 1-58.

78. Marcus RL, Addison O, Kidde JP, et al. Skeletal muscle fat infiltration: impact of age, inactivity, and exercise. J Nutr Health Aging 14 (2010): 362-366.

79. Park YM, Myers M, Vieira-Potter VJ. Adipose tissue inflammation and metabolic dysfunction: role of exercise. Mo Med 111 (2014): 65-72.

80. Tall AR, Yvan-Charvet L. Cholesterol, inflammation and innate immunity. Nat Rev Immunol 15 (2015): 104-116.

81. Ferraro E, Giammarioli AM, Chiandotto S, et al. Exercise-induced skeletal muscle remodeling and metabolic adaptation: redox signaling and role of autophagy. Antioxid Redox Signal 21 (2014): 154-176.

82. Tuttle CSL, Thang LAN, Maier AB. Markers of inflammation and their association with muscle strength and mass: A systematic review and meta-analysis. Ageing Research Reviews 64 (2020): 101185.

83. Perandini LA, Chimin P, Lutkemeyer DdS, et al. Chronic inflammation in skeletal muscle impairs satellite cells function during regeneration: can physical exercise restore the satellite cell niche? The FEBS Journal 285 (2018): 1973-1984.

84. Satriano J. Arginine pathways and the inflammatory response: Interregulation of nitric oxide and polyamines: Review article. Amino Acids 26 (2004): 321-329.

85. Bisserier M, Shanmughapriya S, Rai AK, et al. Cell-Free Mitochondrial DNA as a Potential Biomarker for Astronauts' Health. J Am Heart Assoc 10 (2021): e022055.

86. Nguyen HP, Tran PH, Kim KS, et al. The effects of real and simulated microgravity on cellular mitochondrial function. npj Microgravity 7 (2021).

87. Qiu J, Fang Q, Xu T, et al. Mechanistic Role of Reactive Oxygen Species and Therapeutic Potential of Antioxidants in Denervation- or Fasting-Induced Skeletal Muscle Atrophy. Frontiers in Physiology 9 (2018).

88. Nakanishi N, Tsutsumi R, Hara K, et al. Urinary Titin N-Fragment as a Biomarker of Muscle Atrophy, Intensive Care Unit-Acquired Weakness, and Possible Application for Post-Intensive Care Syndrome. Journal of Clinical Medicine 10 (2021): 614.

89. Reid MB, Moylan JS. Beyond atrophy: redox mechanisms of muscle dysfunction in chronic inflammatory disease. J Physiol 589 (2011): 2171-2179.

90. Zhang YG, Niu JT, Wu HW, et al. Actin-Binding Proteins as Potential Biomarkers for Chronic Inflammation-Induced Cancer Diagnosis and Therapy. Anal Cell Pathol (Amst) 2021 (2021): 6692811.

91. Du J, Wang X, Miereles C, et al. Activation of caspase-3

Hoangvi Le, et al., J Ortho Sports Med 2024
DOI:10.26502/josm.511500161

is an initial step triggering accelerated muscle proteolysis in catabolic conditions. Journal of Clinical Investigation 113 (2004): 115-123.

92. Huang Z, Zhu J, Sun J, et al. Effect of mammalian target of rapamycin signaling pathway on nerve regeneration. Biotarget 2 (2018): 18-18.

93. Sandri M, Sandri C, Gilbert A, et al. Foxo transcription factors induce the atrophy-related ubiquitin ligase atrogin-1 and cause skeletal muscle atrophy. Cell 117 (2004): 399-412.

94. Okada R, Fujita S-I, Suzuki R, et al. Transcriptome analysis of gravitational effects on mouse skeletal muscles under microgravity and artificial 1 g onboard environment. Scientific Reports 11 (2021): 9168.

95. Cadena SM, Zhang Y, Fang J, et al. Skeletal muscle in MuRF1 null mice is not spared in low-gravity conditions, indicating atrophy proceeds by unique mechanisms in space. Scientific Reports 9 (2019): 9397.

96. Kakareka K. Transcriptional Regulation of Skeletal Muscle Atrophy-Induced Gene Expression by Muscle Ring Finger-1 and Myogenic Regulatory Factors. UNF Graduate Theses and Dissertations (2017).

97. Schmidt F, Kny M, Zhu X, et al. The E3 ubiquitin ligase TRIM62 and inflammation-induced skeletal muscle atrophy. Critical Care 18 (2014): 545.

98. Lehti TM, Silvennoinen M, Kivelä R, et al. Effects of streptozotocin-induced diabetes and physical training on gene expression of titin-based stretch-sensing complexes in mouse striated muscle. American Journal of Physiology-Endocrinology and Metabolism 292 (2007): E533-E542.

99. Swist S, Unger A, Li Y, et al. Maintenance of sarcomeric integrity in adult muscle cells crucially depends on Z-disc anchored titin. Nature Communications 11 (2020): 4479.

100. Peng J, Raddatz K, Labeit S, et al. Muscle atrophy in Titin M-line deficient mice. Journal of Muscle Research and Cell Motility 26 (2006): 381-388.

101. Ji Y, Li M, Chang M, et al. Inflammation: Roles in Skeletal Muscle Atrophy. Antioxidants (Basel) 11 (2022).

102. Huang Z, Fang Q, Ma W, et al. Skeletal Muscle Atrophy Was Alleviated by Salidroside Through Suppressing Oxidative Stress and Inflammation During Denervation. Front Pharmacol 10 (2019): 997.

103. Pan M, Liu J, Huang D, et al. FoxO3 Modulates LPS-Activated Hepatic Inflammation in Turbot (Scophthalmus maximus L.). Frontiers in Immunology 12 (2021).

104. Baehr LM, Hughes DC, Lynch SA, et al. Identification of the MuRF1 Skeletal Muscle Ubiquitylome Through Quantitative Proteomics. Function 2 (2021).

105. Nakanishi N, Tsutsumi R, Hara K, et al. Urinary Titin N-Fragment as a Biomarker of Muscle Atrophy, Intensive Care Unit-Acquired Weakness, and Possible Application for Post-Intensive Care Syndrome. J Clin Med (2021).

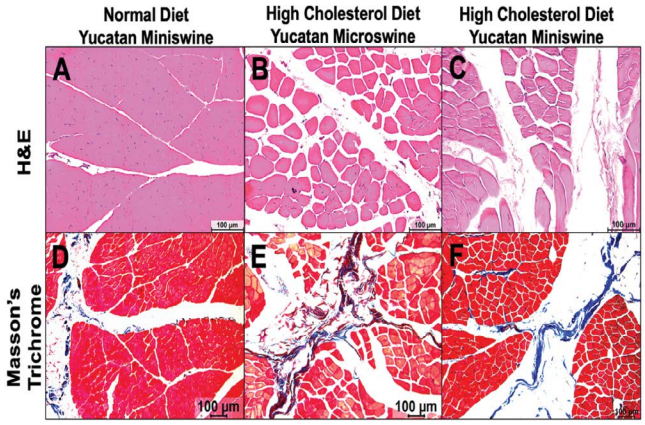

Figure S1: Hematoxylin & Eosin (A–C) and Masson's Trichrome (D–E) staining of normal Yucatan miniswine supraspinatus, hypercholesterolemic Yucatan microswine supraspinatus, and hypercholesterolemic Yucatan miniswine supraspinatus. Supraspinatus muscle tissues in hypercholesterolemic Yucatan miniswine revealed fatty infiltration, muscle mass degeneration, increased inflammation, and increased collagen deposition.

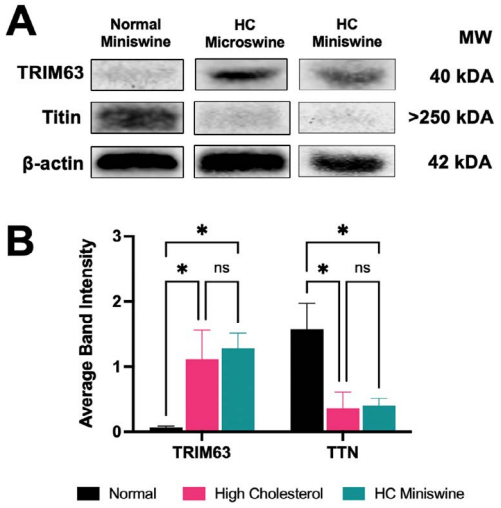

Figure S2: TRIM63 and titin gene expression and protein expression between normal miniswine supraspinatus muscle, hypercholesterolemic microswine supraspinatus muscle (red color), and hypercholesterolemic miniswine supraspinatus muscle (green color). (A) Western blot of TRIM63 and titin in normal and both high cholesterol skeletal muscle; Beta-actin is the loading control. (B) Average band intensity of TRIM63 and titin protein. The statistical analysis used was 1-way ANOVA. The data are presented as mean ± SEM (n=7 in each group). *p<0.05, **p<0.01, ***p<0.001, ****p<0.0001. HC = High Cholesterol. Supraspinatus muscle tissues in hypercholesterolemic Yucatan miniswine revealed increased TRIM63 expression and decreased titin expression.

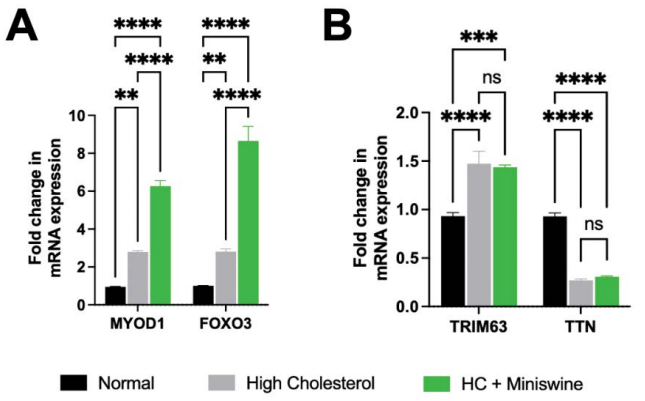

Figure S3: Skeletal muscle atrophy gene expression between normal miniswine supraspinatus muscle, hypercholesterolemic microswine supraspinatus muscle (grey color), and hypercholesterolemic miniswine supraspinatus muscle (green color). (A) Fold change in mRNA expression of MYOD1 and FOXO3. (A) Fold change in mRNA expression of TRIM63 and TTN. The statistical analysis used was 1-way ANOVA. The data are presented as mean ± SEM (n = 7 in each group). *p<0.05, **p<0.01, ***p<0.001, ****p<0.0001. HC = High Cholesterol. Supraspinatus muscle tissues in hypercholesterolemic Yucatan miniswine revealed increased MYOD1, FOXO3, and MURF1/TRIM63 expression and decreased titin expression.

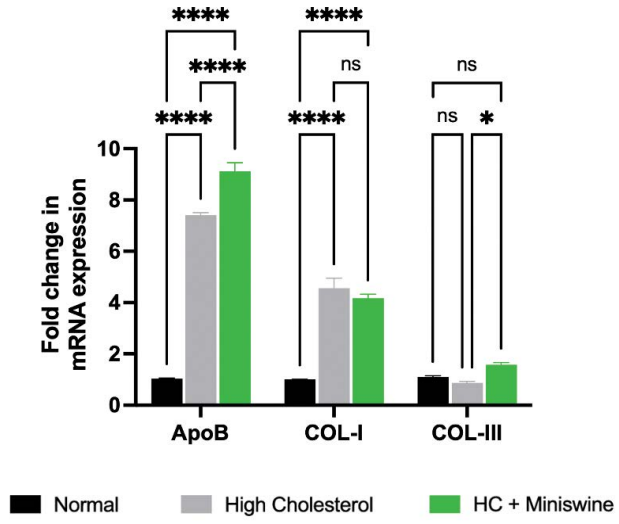

Figure S4: ApoB, COL-I, and COL-III gene expression between normal miniswine supraspinatus muscle, hypercholesterolemic microswine supraspinatus muscle (grey color) and hypercholesterolemic miniswine supraspinatus muscle (green color). (Statistical analysis used was 1-way ANOVA. The data are presented as mean ± SEM (n = 7 in each group). *p<0.05, **p<0.01, ***p<0.001, ****p<0.0001. HC = High Cholesterol. Supraspinatus muscle tissues in hypercholesterolemic Yucatan miniswine revealed increased ApoB, collagen I, and collagen III expression.